

# Three-dimensional Surface Reconstruction of Aircraft Component using Digital Photogrammetry

Tho, N.T.<sup>1</sup>, Suada, M.G.<sup>1</sup>, Dirgantara, T.<sup>1</sup>, and Putra, I.S.<sup>1\*</sup>

<sup>1</sup>*Lightweight Structure Research Group  
Bandung Institute of Technology, Bandung, Indonesia, 40132  
0062 224254016, 0062 222508519, isp@aero.pauir.itb.ac.id*

In this paper, the application of photogrammetry to accurately reconstruct three-dimensional shape of an aircraft component is presented. This technique, which has matured significantly throughout the years, is originally an optical method to measure distances with high accuracy. In this work, images of the object are taken from several positions using single digital camera. Circular markers are distributed over the surfaces of the object in order to improve the accuracy of the reconstructed object. The accuracy of the reconstruction process is checked by comparing several measurements using caliper with the distance obtained by photogrammetry. The results show that the differences is less than 0.1%.

## Keywords :

Surface reconstruction, photogrammetry, circular targets, point cloud.

## 1. Introduction

In the last two decades, there have been a number of advances in the efficiency and effectiveness of image-based metrology systems. The use of digital images and digital transmission of images, the expansions in image resolution provided by new CCD arrays, the rapid measurement of targets and the increasing sophistication of software for data analysis and geometric fitting are all factors that have contributed to the gains in efficiency and effectiveness. One of the most popular image-based techniques used in industry in photogrammetry.

Photogrammetry is a technique of measuring objects (2-D or 3-D) from photographs. Its most important feature is the fact that the objects will be measured without being touched. Therefore, the term “remote sensing” is used by some authors instead of “photogrammetry”. The goal of photogrammetry is to determine geometric properties of the three-dimensional (3-D) world from images. Navigation of autonomous vehicles, object recognition, reverse engineering and synthesis of virtual environment are some of its applications which reconstruct a 3-D model of the scene from a moving camera [1].

In this paper, the surface reconstruction of an aircraft component is performed. Its images are captured by a single digital camera at different positions in space. Then, corresponding features will be matched (or referenced) from image to image. The matching performance is significantly increased with the use of circular markers, which are distributed over all surfaces of the object. Triangulation, which may be formulated as a least-squares minimization, will recover the position of a point in space given its position in two or more images taken with cameras with known calibration and pose. Finally, 3-D coordinates of the features and camera poses are refined using the bundle adjustment [7, 8] which is a non-linear optimization of triangulation.

A number of surface reconstruction works have been studied such as that of a five-meter inflatable space antenna under a NASA project in 2001 by Pappa [9]. One year later, Pappa and his colleagues applied photogrammetry to reconstruct spacecraft structures [10]. The procedures presented in those projects are only consistent with commercial softwares. They showed that the average measurement precision for more than 500 markers on the

---

\* Corresponding Author. E-mail : isp@aero.pauir.itb.ac.id  
Phone : +62-22-4254016, Fax. : +62-22-2508519

antenna surface was less than 0.020 inches in-plane and approximately 0.050 inches out-of-plane. The precision presented in table 1 reaches 0.0109 millimeters in average, which is good compared to the results reported in [9, 10].

## 2. Methodology

In this section, brief mathematical formulation related to this work is introduced.

A pinhole camera is modeled by its *optical center*  $\mathbf{O}$  and its *image plane*  $\mathbf{I}$ . A 3-D point  $\mathbf{M}$  is projected into an image point  $\mathbf{m}$  given by the intersection of  $\mathbf{I}$  and the line containing  $\mathbf{O}$  and  $\mathbf{M}$ . For simplicity, let  $\mathbf{M} = (X, Y, Z)$  be the coordinates of point  $\mathbf{M}$  in the world reference frame and  $\mathbf{m} = (x, y)$  be the pixel coordinates of point  $\mathbf{m}$ . In homogeneous (or projective) coordinates:

$$\tilde{\mathbf{m}} = \begin{pmatrix} x \\ y \\ 1 \end{pmatrix} \quad \tilde{\mathbf{M}} = \begin{pmatrix} X \\ Y \\ Z \\ 1 \end{pmatrix} \quad (1)$$

The transformation from  $\tilde{\mathbf{M}}$  to  $\tilde{\mathbf{m}}$  is given by the *perspective projection matrix*  $\mathbf{P}$ :

$$\lambda \tilde{\mathbf{m}} = \mathbf{P} \tilde{\mathbf{M}} \quad (2)$$

where  $\lambda$  is a scale factor. The camera is then modeled by its matrix  $\mathbf{P}$ , which can be decomposed by QR factorization:

$$\mathbf{P} = \mathbf{K} [\mathbf{R} | \mathbf{t}] \quad (3)$$

The *camera matrix*  $\mathbf{K}$  depends only on the *intrinsic parameters* of the camera, and has the following form:

$$\mathbf{K} = \begin{bmatrix} f_x & s & x_0 \\ 0 & f_y & y_0 \\ 0 & 0 & 1 \end{bmatrix} \quad (4)$$

where  $f_x = fk_x$ ,  $f_y = fk_y$  are the *effective focal length* in horizontal and vertical axis, respectively ( $f$  is the focal length in millimeters,  $k_x$  and  $k_y$  are the effective number of pixels per millimeter along the  $x$ - and  $y$ -axes),  $(x_0, y_0)$  are the coordinates of the *principal point*, determined by the orthogonal projection of  $\mathbf{O}$  onto the plane  $\mathbf{I}$ , and  $s$  is the skew factor.

The camera position and orientation (*extrinsic parameters*) are encoded by a  $3 \times 3$  rotation matrix  $\mathbf{R}$  and a translation vector  $\mathbf{t}$ , representing the rigid transformation that aligns the camera reference frame and the world reference frame.

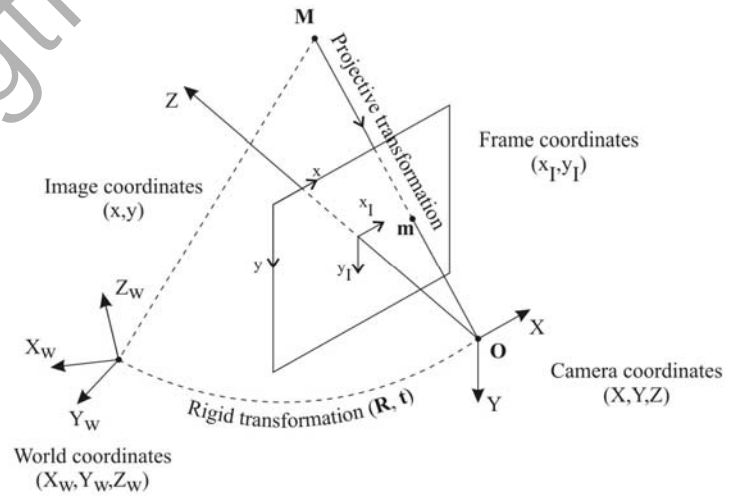


Figure 1. Camera model with coordinate systems

### 2.1 Calibration

A calibration is required to find out all components of the matrix  $\mathbf{K}$  (or intrinsic parameters). A checkerboard of black and white squares is used as the target object to calibrate the camera. The board is placed at different positions to the camera, which is in turn kept stable and unchanged. With the aid of Harris corner detection algorithm [2], the intrinsic parameters of the camera will be recovered [3]. A 30D Canon digital camera with identical zoom lens

Canon EF28-135mm F3.5-5.6 IS USM is used to capture images of the checkerboard and the aircraft component.

## 2.2 Ellipse fitting (target detection) – Pose from ellipses

The aircraft component will be reconstructed based on the center coordinates of the circular targets distributed over its surfaces. Since the images are taken from different orientations, the circular shape of the targets becomes ellipses. Canny edge detection is applied first to extract the edges of the ellipses, and then direct least square ellipse fitting can be used to locate the centers of the ellipses in the image reference frame and the normal vectors orthogonal to the surface at the corresponding centers.

Assume that the general form of any conic is:

$$F(\mathbf{a}, \mathbf{x}) = Ax^2 + Bxy + Cy^2 + Dx + Ey + F = 0 \quad (5)$$

and in matrix form:

$$\mathbf{a} \cdot \mathbf{x} = 0 \quad (6)$$

where  $\mathbf{a} = (A, B, C, D, E, F)^T$  is a vector containing all parameters which can define a conic, and  $\mathbf{x}$  is a vector which stores coordinates used in ellipse fitting. The fitting of a general conic may be approached by minimizing the sum of squared algebraic distances:  $\min \left\{ d(\mathbf{a}) = \sum_{i=1}^n F(\mathbf{x}_i) \right\}$ . By introducing the quadratic constraint  $B^2 - 4AC = -1$ , the vector  $\mathbf{a}$  can be computed through a system of equations (see [4] for more details). The most important information from ellipse fitting is the coordinates of its center which is easily determined by rewriting general equation in canonical form:

$$\left( \frac{x-x_0}{a} \right)^2 + \left( \frac{y-y_0}{b} \right)^2 = \left( \frac{x + \frac{D'}{2A'}}{\sqrt{\frac{F'}{A'}}} \right)^2 + \left( \frac{y + \frac{E'}{2C'}}{\sqrt{\frac{F'}{C'}}} \right)^2 = 1 \quad (7)$$

where  $A' = Ac^2 - Bcs + Cs^2$ ;  $C' = As^2 + Bcs + Cc^2$ ;  $D' = Dc - Es$ ;  $E' = Ds + Ec$ ;  $F' = -F + \frac{D'^2}{4A'} + \frac{E'^2}{4C'}$ ;

$c = \cos \theta$ ;  $s = \sin \theta$  and  $\theta = \frac{1}{2} \arctan \frac{B}{C-A}$ .

## 2.3 Point cloud from sequence of images

Corresponding center points of ellipses on every images of the sequence will be referenced from one to another in order to calculate the fundamental matrix  $\mathbf{F}$ . Then, camera position (or translation vector  $\mathbf{t}$ ) and orientation (or rotation matrix  $\mathbf{R}$ ) are extracted from  $\mathbf{F}$  (see [5]). In this method, the object frame is aligned with the first camera (i.e. coincide with the camera frame). The second position of the camera is chosen so that the epipolar geometry corresponds to the retrieved  $\mathbf{F}_{21}$ :

$$\mathbf{P}_1 = \mathbf{K}[\mathbf{I}_{3 \times 3} \mid \mathbf{0}_{3 \times 3}]; \quad \mathbf{P}_2 = \mathbf{K}[\mathbf{R}_{21} \mid \mathbf{t}_{21}] \quad (8)$$

The projection matrix of the third image is then  $\mathbf{P}_3 = \mathbf{K}[\mathbf{R}_{21} \mathbf{R}_{32} \mid \mathbf{R}_{21} \mathbf{t}_{32} + \mathbf{t}_{21}]$ , and so on. When all projection matrices  $\mathbf{P}$  and normalized image coordinates  $\mathbf{m}$  are known, the 3-D points  $\mathbf{M}$  will be computed by Eq. (4) through triangulation [6]. Minimization of the distances between the reprojected 3-D points and the image points should be carried out. The set of such points  $\mathbf{M}$  creates a point cloud of the 3-D surface.

## 2.4 Sparse bundle adjustment

Bundle adjustment (BA) is the last step to refine a visual reconstruction to produce *jointly optimal* 3-D structure and viewing parameter estimates. *Optimal* means that the parameter estimates are found by minimizing some cost function that quantified the model fitting error, and *jointly* that the solution is simultaneously optimal with respect to both structure and camera variations [7]. BA is really a large sparse geometric parameter estimation problem, the parameters being the combined 3-D feature coordinates, camera positions and orientations. BA minimizes the reprojection error with respect to all 3-D point and camera parameters, specially:

$$\min_{\mathbf{a}_j, \mathbf{b}_i} \sum_{i=1}^n \sum_{j=1}^m d(\mathbf{Q}(\mathbf{a}_j, \mathbf{b}_i), \mathbf{x}_{ij})^2 \quad (9)$$

where  $\mathbf{a}_j$  is a vector containing all (intrinsic and extrinsic) parameters and initial estimated pose of the camera  $j$ ,  $\mathbf{b}_i$  is a vector containing parameters of the  $i$ -th 3-D point,  $\mathbf{Q}(\mathbf{a}_j, \mathbf{b}_i)$  is the predicted projection of point  $I$  on image  $j$  and  $d(x, y)$  denotes the Euclidean distance between the inhomogeneous image points represented by  $\mathbf{x}$  and  $\mathbf{y}$ . The expression (9) can be treated as a non-linear minimization based on Levenberg-Marquardt algorithm by solving the *normal equations*:

$$\mathbf{J}^T \mathbf{J} \delta = -\mathbf{J}^T \varepsilon \quad (10)$$

where  $\mathbf{J}$  is the Jacobian of the error function,  $\delta$  is the update to the parameter vector and  $\varepsilon$  is the difference between the real and the initially estimated values [8]. Note that if  $\kappa$  and  $\lambda$  are respectively the dimensions of each  $\mathbf{a}_j$  and  $\mathbf{b}_i$ , the total number of minimization parameters in (9) equals  $m\kappa + n\lambda$  and is therefore large even for moderately sized BA problems.

In short, the algorithm of surface reconstruction using digital photogrammetry is summarized in the block-diagram below:

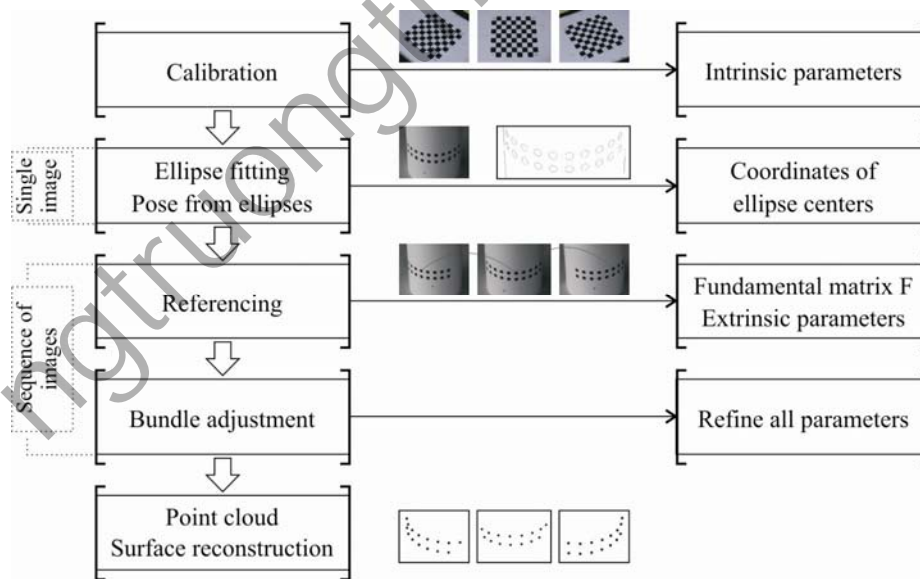


**Figure 2. Outline of 3-D surface reconstruction algorithm**

### 3 Results

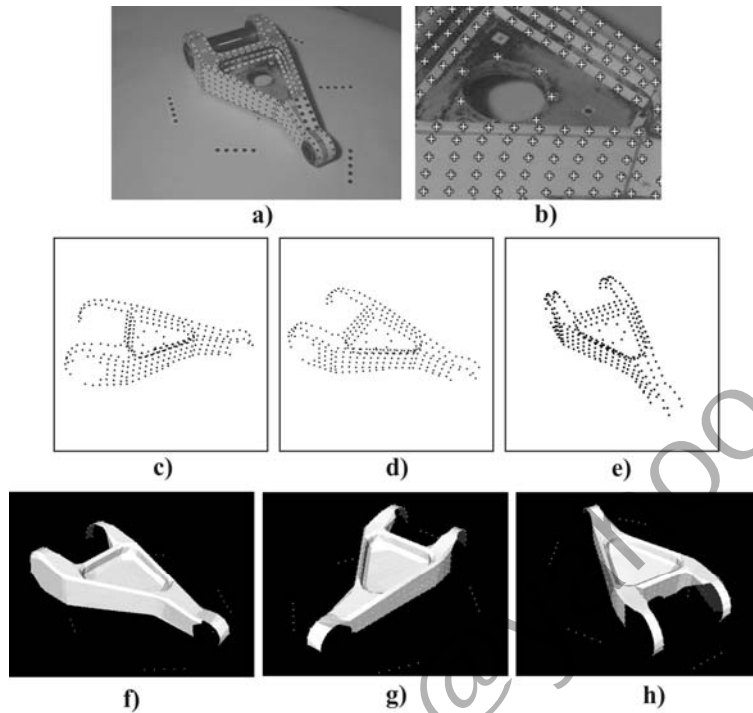


**Figure 3.** a) b) Aircraft component with detected circular targets  
 c) d) e) Reconstructed point cloud of the component  
 f) g) h) Surface reconstruction based on point cloud

Distances (mm)	by Direct	by	Absolute	Relative
	Measurement (mm)	Photogrammetry (mm)	differences (mm)	differences (%)
e1	8.55	8.5446	0.0054	0.0632
e2	8.70	8.7243	0.0243	0.2793
e3	36.70	36.7003	0.0003	0.0008
e4	36.85	36.8523	0.0023	0.0062
e5	13.10	13.0776	0.0224	0.1710
Average:	20.78	20.7691	0.0109	0.0525

**Table 1. Measurement precision for 5 specific thicknesses of the component**

### 4 Discussions

The edge thicknesses of the aircraft component, labeled from e1 to e5, are measured by a caliper of 0.05 mm. precision (direct measurement). The corresponding distances which are joined by reconstructed points of the point cloud (by photogrammetry) are computed and compared to those of direct measurement. The higher the precision of the measuring instrument is, the more accurate the results are. The precision of the method using digital photogrammetry which falls into the interval between 0.0003 and 0.0243 mm, has a mean value of 0.0109 mm. In

percentage, this interval is approximately from 0.001 to 0.3% which is good enough compared to the results given in [9, 10].

## 5 Conclusion

Photogrammetry is a leading candidate technology for measuring the static shape of complicated-shape structures. It offers the simplicity of taking photographs coupled with good to excellent measurement precision. This paper discussed a method of five main steps to create 3-D surfaces model of an aircraft component. The key idea is the use of circular targets on the object's surfaces. The results show that the method meets all desired objectives, especially the measurement precision (0.0525% in average).

## Acknowledgments

This research is funded by JICA – AUN/SEED-Net Collaborative Research Project 2006 – 2008. JICA – AUN/SEED-Net scholarship for the first author is also gratefully acknowledged.

## References

- [1] A. Fusiello (2000), Uncalibrated Euclidean reconstruction: a review, *Image and Vision Computing*, Vol. **18**, 555 – 563.
- [2] Trucco, E. and Verri, A. (1998), *Introductory Techniques for 3-D Computer Vision*, New Jersey: Prentice-Hall, Inc., 82 – 85.
- [3] Bouguet, J.Y. (2007): Camera calibration toolbox for Matlab, [http://www.vision.caltech.edu/bouguetj/calib\\_doc/](http://www.vision.caltech.edu/bouguetj/calib_doc/)
- [4] Fitzgibbon, A., Pilu, M. and Fisher, R.B. (1999), Direct least square fitting of ellipses, *IEEE Transaction on pattern analysis and machine intelligence*, Vol. **21**, 476 – 480.
- [5] Hartley, R.I. and Zisserman, A. (2003), *Multiple View Geometry in Computer Vision*, Cambridge University Press, 279 – 308.
- [6] Hartley, R.I. and Sturm, P. (1997), Triangulation, *Computer Vision and Image Understanding*, Vol. **68**, No. 2, 146 – 157.
- [7] B. Triggs, P. McLauchlan, R. Hartley and A. Fitzgibbon (1999), Bundle Adjustment – A Modern Synthesis, *International Workshop on Vision Algorithms: Theory and Practice*, 298 – 372.
- [8] Manolis I.A. Lourakis and Antonis A. Argyros (2004), The design and implementation of a generic sparse bundle adjustment software package based on the Levenberg-Marquardt algorithm, Technical Report, FORTH-ICS/TR-340.
- [9] Pappa, R. S., Giersch, L. R. and Quagliaroli, J. M. (2001), Photogrammetry of a 5 m inflatable space antenna with consumer grade digital cameras, *Experimental Techniques*, Vol. **25**, No. 4, 21 – 29.
- [10] Pappa, R.S., Jones, T.W., Black, J.T., Walford, A., Robson, S. and Shortis, M.R. (2002), Photogrammetry methodology development for Gossamer spacecraft structures, Technical Memorandum, NASA/TM-2002-211739